A Multiresolution Framework to MEG/EEG Source Imaging

Laurence Gavit, Sylvain Baillet*, *Member, IEEE*, Jean-François Mangin, Jérémie Pescatore, and Line Garnero, *Member, IEEE*

***Abstract*—A new method based on a multiresolution approach for solving the ill-posed problem of brain electrical activity reconstruction from electroencephaloram (EEG)/magnetoencephalogram (MEG) signals is proposed in a distributed source model. At each step of the algorithm, a regularized solution to the inverse problem is used to constrain the source space on the cortical surface to be scanned at higher spatial resolution. We present the iterative procedure together with an extension of the ST-maximum *a posteriori* method [1] that integrates spatial and temporal *a priori* information in an estimator of the brain electrical activity. Results from EEG in a phantom head experiment with a real human skull and from real MEG data on a healthy human subject are presented. The performances of the multiresolution method combined with a nonquadratic estimator are compared with commonly used dipolar methods, and to minimum-norm method with and without multiresolution. In all cases, the proposed approach proved to be more efficient both in terms of computational load and result quality, for the identification of sparse focal patterns of cortical current density, than the fixed scale imaging approach.**

***Index Terms*—EEG/MEG, imaging, inverse problem, multiresolution, regularization.**

I. Introduction

ELECTROENCEPHALOGRAPHY (EEG) and magnetoencephalography (MEG) offer excellent time resolution only limited by the analog-to-digital sampling rate, in the 1–10 ms range. However, spatial resolution is limited as very different source patterns can lead to the same EEG and MEG measurements. The inverse problem consisting in extracting a source map from the data is thus said to be ill posed, having no unique solution and being numerically instable. Different methods have been proposed to solve this problem.

The dipolar approach consists in searching one or few dipole locations and orientations the forward solution of which is a best fit (generally in the least-square sense) to measurements [2]. These techniques are simple to implement but do not produce an explicit description of the extension of the cortical activity. Moreover the estimation of the number of dipoles to fit, i.e., the number of active areas, is left to the user.

Another approach first introduced by Hämäläinen *et al.* [3] is the distributed source model consisting in a spatial sampling of the whole cerebral volume [4], or restricted to the cortical surface [5]. In this approach, the linear operator relating the data to the source amplitudes is badly conditioned. A simple estimate of the current source amplitude can be obtained as the minimum least-square solution under constraints of minimum norm of current amplitudes. This approach provides very smooth-looking intensity patterns but fails to recover focal activities.

In [1] and [6], the inverse problem is regularized through a Bayesian approach which allows the introduction of *a priori* information in the regularization scheme (see Section II-B). Unfortunately this approach is limited by the computational burden of estimating the amplitude of thousands of sources to be reconstructed from only about 200 simultaneous data samples.

Iterative focalization approaches found in the literature are poised to solve this underdetermined problem. FOCUSS [7] for instance, is based on a recursive minimum-norm approach. A repeated weighted procedure concentrates the solution in focal regions; weights are applied to the forward gains of the sources according to their moments at the previous iteration, hence enhancing the contribution of sources with larger amplitudes at the next iteration step. A similar technique is exposed in [8] and proposes a generalization of LORETA [4] by locally adapting the degree of regularization. These minimum-norm procedures end up with only a small number of remaining nonzero elements but require multiple recursions before convergence. Hence, practical computational time and memory limitations necessitate the use of linear estimators. Because the dimension of the source space is fixed along iterations, these methods would not reduce the computational load for more sophisticated source models.

Hence, another approach consists in iteratively reducing the search space around emerging active areas: Srebro proposed an iterative scheme to limit the head volume to be searched at each step. The estimation of the source amplitudes is done with a least-square linear estimator. In [9], a single search area is determined by building an ellipsoid centered at the center of gravity of the activity at the previous iteration. However, a crucial shortcoming of this method consists in estimating the current density within a single cortical subvolume with fixed spatial resolution.

We propose here a multiresolution iterative procedure in order to deal at each step with a constant number of dipoles distributed in a restricted area but at an increasing spatial resolution. As an extension to Srebro's work, we build several

Manuscript received August 10, 2000; revised July 2, 2001. *Asterisk indicates corresponding author.*

L. Gavit and L. Garnero are with the Cognitive Neuroscience and Brain Imaging Laboratory, CNRS UPR 640, La Salpetriere Hospital, 75651 Paris, France.

*S. Baillet with the Cognitive Neuroscience and Brain Imaging Laboratory, CNRS UPR 640, La Salpetriere Hospital, 47 Blvd. de l'Hopital, 75651 Paris, France (e-mail: sylvain.baillet@chups.jussieu.fr).

J.-F. Mangin is with the SHFJ/CEA, Orsay, France.

J. Pescatore is with the ENST and CNRS UPR 640, Paris, France.

Publisher Item Identifier S 0018-9294(01)08272-6.

ellipsoids instead of a unique area around all the activity centers and define the new source space at their intersection with the cortical surface. We also extend a more sophisticated regularization strategy than the one used by Srebro: our regularization procedure extends Baillet's *et al.* method [10] to multiresolution source imaging with enhanced convergence properties to a unique solution.

The paper is divided as follows: in Section II-A, we recall the formalism used to solve the inverse problem with a distributed source model, and then describe the multiresolution process. In Section II-B, we present the regularization technique that was used and the realistic constraints integrated in the multiresolution scheme. Finally, we present some results in Section III obtained from EEG measurements on a phantom head where single sources were successively activated, and from real MEG data collected from a somatosensory experiment with a healthy human subject. In both cases, the aim was to reconstruct the underlying activity and to compare the performances of the multiresolution method to some alternative methods.

II. METHOD

A. Multiresolution Approach

In a distributed source model using a distribution of current dipoles with given locations and orientations resulting from a segmentation of structural magnetic resonance imaging (MRI) of the brain, source amplitudes can be represented in a column vector J_n. The inverse problem of recovering source magnitudes from EEG and/or MEG measurements can then be written in a way that is standard for many linear image reconstruction problems in a noisy environment

$$M_n = GJ_n + b_n \tag{1}$$

where M_n is a N_M column vector containing EEG and/or MEG measurements at time n, and G is a $N_M \times N$ gain matrix which depends on the head model, the source set pattern, and the sensor locations. J_n is an N column vector containing the nth time sample of dipole magnitudes. The model also contains an additive noise process b_n. Solving the *inverse problem* consists in obtaining an estimate $\hat{J}_n$ of the true object J_n from the data vector M_n.

Classical cortical distributed methods aim at determining the magnitude of dipoles, perpendicular to the cortical surface and located at each node of a mesh representing either the interface between white and gray brain matters or the cortical surface. This mesh is obtained through a segmentation of structural MRI and generally contains a large number of nodes ($\sim 10^4$). Thus, despite their elegant formalism, distributed methods are numerically very demanding because of the size of J_n to be estimated, when such a realistic anatomy description is used. In order to overcome this difficulty, we introduce the following multiresolution scheme for iterative distributed source estimation.

At every resolution but the highest, the number of source candidates is limited to N', a number much smaller than the total number of possible sources defined as the nodes of the high-resolution tessellation of the cortical surface. The iterative procedure proceeds to the successive definition of—possibly multiple—subspaces of locally increasing source density based on the source intensity distribution, estimated at the previous step. The iterative procedure runs along the following lines.

1) Initialization: source amplitude estimation at the lowest resolution.
2) Definition of the new source space:
   a) Selection of the source with largest amplitude as the centroid of a new local search space.
   b) Estimation of the spatial extension of the activity about this centroid as an ellipsoid of interest.
   c) Proceed to the next largest source above a threshold left in the source space and repeat 2)b).
3) Definition of the new source space at higher resolution within the ellipsoid(s) of interest.
4) Source amplitude estimation limited to the source space defined in 3) using some regularization adapted to the resolution.
5) Repeat 2)–4) until amplitude estimation is done at the highest resolution.

Let us now describe these different steps.

Step 2): At iteration k, step 2) consists in the estimation of both the number of possible active regions and their spatial extension around a centroid of maximum of intensity. Following the selection of the source of largest amplitude, as found at iteration $k-1$, the extension of the local current density around this location is estimated via the definition of an ellipsoid of interest which parameters are set following a singular value decomposition (SVD) of the $N \times 3 \hat{J}_n^{k-1}$-weighted source coordinates:

$$X_J = \Delta J \cdot X \tag{2}$$

with

$$\Delta J = \frac{\operatorname{diag}\left(\left|\hat{J}_n^{k-1}\right|\right)}{\left\|\hat{J}_n^{k-1}\right\|} \tag{3}$$

where $\hat{J}_n^{k-1}$ refers to the estimate of J_n at iteration $k-1$ and $\operatorname{diag}(\hat{J}_n^{k-1})$ is a diagonal matrix which nonzero elements are the components of $|\hat{J}_n^{k-1}|$. The SVD decomposition of the transposed matrix X_J^t can thus be written as follow, the three columns of U giving the three axis directions

$$X_J^t = U \cdot S \cdot V^t \tag{4}$$

where ^{t} stands for matrix transposition. The ellipsoid hemi-diameters are set to the obtained singular values.

This procedure is repeated starting from the source location with the next largest amplitude above a threshold μ, proportional to the standard deviation above the mean value of the distribution $\hat{J}_n^{k-1}$ in the patch, and that does not belong to the previous volumes of interest (VOIs).

Step 3): Once the VOIs are defined, the new source distribution at higher resolution is derived from a uniform subsampling of the high resolution cortical surface at the intersection with the ellipsoids of interest so that the total number of sources reaches N', see Fig. 1.

When several time samples are used for the reconstruction, the focalization procedure at iteration k is carried out for a vector $J_{\max}^k$ built with the maximal components for every

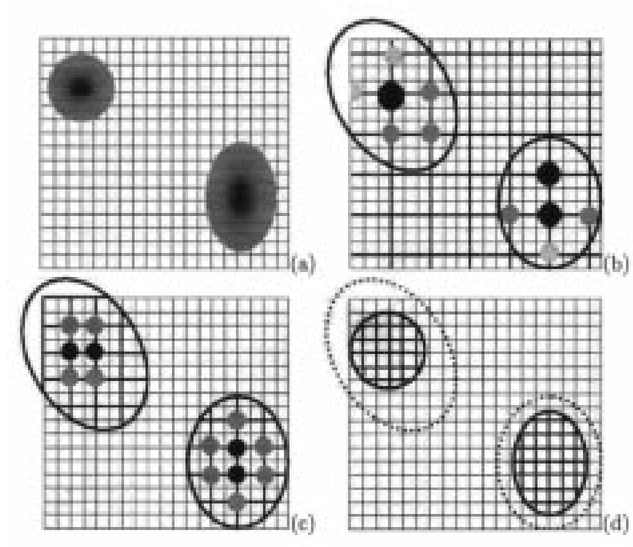

Fig. 1. (a) Example of activity map to be reconstructed on the finest grid. (b) Result of the inverse problem at iteration $k-1$. The grid has been decimated, so that the source space is made of the nodes of the bold grid. Gray levels code the amplitude of the dipoles. Two ellipsoids have been built around the centers of activity. (c) The new source space is defined by decimation of the finest grid, locally in the ellipsoids. Result of the inverse problem at iteration k is shown. (d) New ellipsoids are built, and the maximal resolution is reached: all the nodes in the ellipsoids are considered.

source of $\hat{J}^k$ estimated over time, where $\hat{J}^k$ is a source amplitude matrix which columns are the samples $|\hat{J}_n^k|$ for n in the considered time window.

At intermediate resolution, the dipoles can be far from each other and represent the average activity of a whole region of interest. In this case, regional average activity is modeled by three perpendicular current dipoles. This holds true until maximal resolution is reached, where there is one dipole per mesh node. The normals to the cortical surface can then be used as a constraint for the dipole orientation.

Step 4): The amplitude estimation is performed with a regularization technique as described in the following section.

B. Adaptive Functional and Anatomical Constraints for Regularized Multiresolution Source Imaging

The regularization technique consists in finding the best vector $\hat{J}_n$ according to a given criterion, or cost function to be minimized. This function is a sum of two terms, a least-square error term corresponding to the fidelity to data and a penalization term $L(J_n)$, corresponding to prior knowledge on the source distribution

$$\hat{J}_n = \arg\min_{J_n} U(J_n) \tag{5}$$

where

$$U(J_n) = \|M_n - GJ_n\|_R^2 + \lambda L(J_n) \tag{6}$$

and R is the noise-covariance matrix. λ is a positive scalar that balances the respective contributions to $U(J_n)$ of the data attachment term and the prior term $L(J_n)$ that contains prior information on the source distribution. The weighted least-square is defined as follows:

$$\|M_n - GJ_n\|_R^2 = (M - GJ_n)^t R^{-1} (M - GJ_n). \tag{7}$$

Whether the regularization operator $L(\cdot)$ is quadratic or not, depends on the nature of the priors taken into account. In the classical Tikhonov approach [11], $L(\cdot)$ is the L_2 norm of the object to be estimated but this leads to unrealistic over-smoothed intensity solutions. To obtain more realistic solutions, Markov random fields models of the source space can be used leading to nonquadratic formulation of the priors [12]. These models have been used in EEG/MEG source imaging in [1] and [6].

The focalization process is independent of the chosen regularization technique. Here, we present a nonlinear source estimation method derived from [1]. Supplementary *a priori* information on the source distribution to be estimated is introduced in order to recover focal source clusters in the source image. A first assumption holds that the source magnitude pattern is made of areas with smooth intensity changes that may be separated by higher jumps in source amplitude: this situation occurs for instance between adjacent but functionally *nonrelated* cortical areas, e.g., the ones on both sides of a sulcus. Moreover, it can be safely considered that relevant frequencies of massive neural electrical activity are inferior to 100 Hz. Since measurements are oversampled, it is also assumed that dipole magnitude evolves smoothly with time. As previously explained, only when sources are closer to each other, i.e., at the maximal resolution, precise anatomical assumptions on the source space are acceptable. Therefore, two successive strategies are adopted. The first one at intermediate resolutions and the second one at maximal resolution.

As in [1], we explicit the prior term as

$$L(J_n) = L_s(J_n) + L_t(J_n) \tag{8}$$

where L_s stands for the spatial prior term and L_t for the temporal prior term.

At each resolution, a temporal neighborhood containing the time sample preceding each source is designed. A quadratic cost function is used for the temporal prior term. Assuming that $\hat{J}_{n-1}$ and $\hat{J}_n$ are similar to each other, the orthogonal projection of $\hat{J}_n$ on the hyperplane perpendicular to $\hat{J}_{n-1}$ is "small." Thus, $L_t(J_n)$ can be written as

$$L_t(J_n) = \|P_{n-1} J_n\|^2 \tag{9}$$

where P_{n-1} is the projector onto the hyperplane perpendicular to $\hat{J}_{n-1}$.

At intermediate resolution, L_s is written as a sum of potentials

$$L_s(J_n) = \sum_{i=1}^{N} \phi(J_n^i) \tag{10}$$

where J_n^i is the ith component of vector J_n.

Nonquadratic ϕ-functions allow modulated penalization of high amplitude sources. Indeed, ϕ is growing slower than a quadratic function for large amplitudes, whereas it has a quadratic behavior with small amplitudes. Two main families

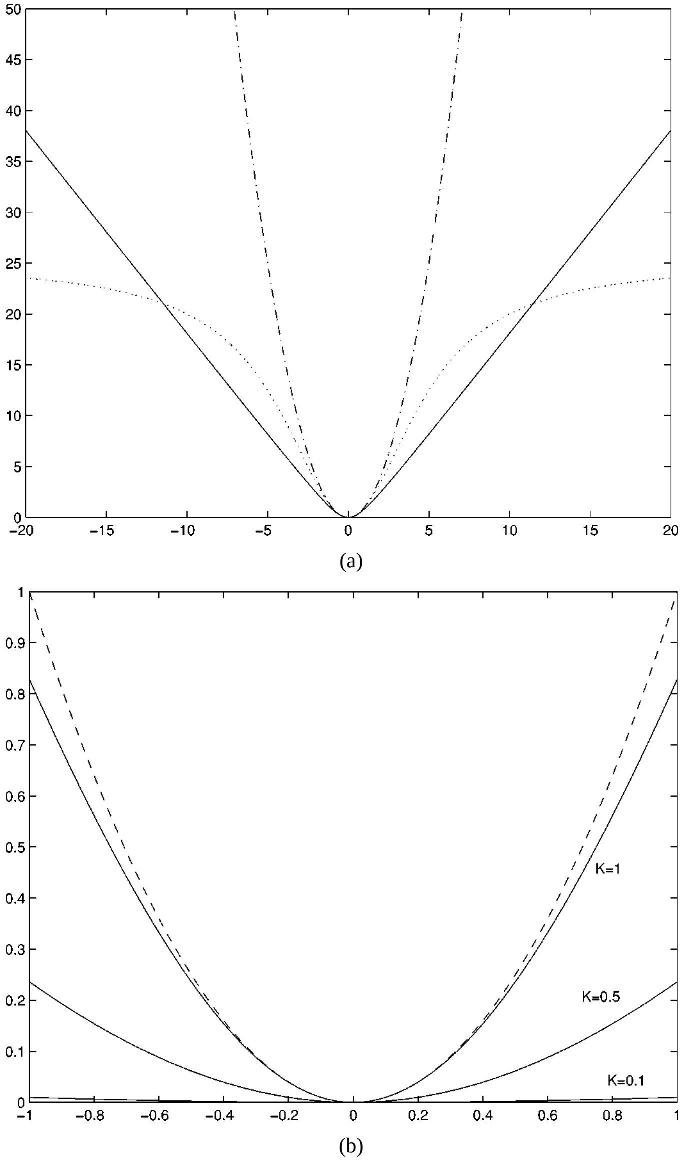

Fig. 2. (a) Prior potential functions for different regularization methods. The dashed–dotted curve is the parabola. The plain curve represents the convex function $\phi_c(u)$ which is an hyperbola branch. The dotted curve represents the nonconvex function $\phi(u)$ so called Lorentz function. It appears clearly that the convex hyperbola branch realizes a good compromise between the strong $L2$-norm regularization and the nonconvex regularization obtained with the Lorentz function. (b) Different shapes of our prior potential functions where K is a scaling factor which tunes the strength of regularization compared with the parabola.

of such functions have been proposed, e.g., [14]. The main difference between them lies in convexity. Nonconvex ϕ-functions allow two very distinct regularization behaviors according to the amplitude value, but introduce convergence problems due to the presence of local minima. On the other hand, convex functions provide a good compromise between efficiency in the regularization procedure and convergence of minimization techniques, see Fig. 2(a) for comparison between different functions. This justifies the use of a convex ϕ-function ϕ_{convex} defined by

$$\phi_{\text{convex}}(u) = 2\sqrt{1 + u^2.K^2} - 2 \qquad (11)$$

Fig. 2(b) shows the variations of the cost functions when K varies. For small values of u, the cost is quadratic whereas large values are associated to a linear cost depending on the value of K used as a discontinuity threshold. This model may be interpreted as follows: this type of priors penalizes large-norm solutions, but to a lesser extent than quadratic penalization. Sources with large amplitudes will emerge from a relatively homogeneous background, whereas a quadratic regularization function will over-smooth the solution. Although K could be chosen locally according to anatomical priors, K is set constant at intermediate resolution for each source, since prior knowledge on the activation location is not available. In this case, K was set to one.

At maximal resolution, sources are close to each other and relevant anatomy-based constraints can be introduced. The idea is to correlate sources that belong to a same functional area, and on the opposite to allow discontinuity between source amplitudes belonging to different functional zones. For this purpose, ϕ is applied to source gradients. A spatial neighborhood system is designed, with the closest nodes on the cortex surface mesh and L_s is then written as a sum of locally calculated potentials

$$L_s(J_n) = \sum_{i=1}^{N} \sum_{\nu=1}^{N_\nu} \phi_\nu^i(\nabla_i^\nu J_n) \qquad (12)$$

∇_i^ν is the gradient operator on sources i and ν amplitudes and N_ν is the number of neighbors of each dipole. In this case

$$\phi_{\text{convex}}(\nabla_i^\nu J_n) = 2\sqrt{1 + (\nabla_i^\nu J_n)^2.K^2} - 2 \qquad (13)$$

and K is chosen locally in accordance with anatomical priors, depending on whether as K-indexed potential functions ϕ_ν^i are applied to gradients between *a priori* correlated dipoles or not. As close sources may be located on opposite walls of the same sulcus, it is essential to index the detection thresholds on the source orientations. Indeed, these sources may be considered to be functionally independent, but may have very similar contribution to data that make them difficult to discriminate in the inverse procedure. Discrimination of intensity jumps between these two sources is facilitated when some prior information explicitly introduces the possibility of such intensity jumps. We chose the definitions used in [10] for the discontinuity threshold

$$K = \alpha.\beta \qquad (14)$$

$$\alpha = 1 - \frac{d_{i\nu}}{\max_{j\in[1\cdots N_\nu]}(d_{ij})} \qquad (15)$$

$$\beta = \frac{1 + \vec{n_i}.\vec{n_\nu}}{2} \qquad (16)$$

where

- $d_{k\nu}$ Euclidian distance between source k and its neighbor ν;
- $\vec{n_k}$ unitary orientation vector of source k;
- α depends on the distance between source k and neighbor ν;
- β index of the orientation discrepancy of the two considered sources.

Both scalars vary in the interval [0,1], so that K bound values correspond to two extreme regularization strategies as shown in Fig. 2(b).

In summary, we adopted two regularization strategies: one at intermediate resolution, and the other at maximal resolution where the potential functions are applied on gradients to take full advantage of anatomical information. In both cases, the ϕ_{convex}-function defined by equation (11) is used. The two criteria to be minimized are, therefore, as follows.

- At intermediate spatial resolution

$$U(J_n) = \|M_n - GJ_n\|_R^2 + \lambda\left(\sum_{i=1}^{N} \phi_{\text{convex}}(J_n^i) + \|P_{n-1}J_n\|^2\right). \quad (17)$$

- At maximal spatial resolution

$$U(J_n) = \|M_n - GJ_n\|_R^2 + \lambda\left(\sum_{i=1}^{N}\sum_{\nu=1}^{N_\nu} \phi_{\text{convex}}\left(\nabla_i^\nu J_n\right) + \|P_{n-1}J_n\|^2\right). \quad (18)$$

These nonquadratic criteria are minimized by a deterministic descent method derived from the ARTUR algorithm described in [15], and convergence is granted by the convexity of the criteria. Initialization is done with a minimum-norm solution, while an empirical adjustment of the hyper-parameter λ is realized.

III. Results

In this section, results from two different experiments are presented. In the first one, EEG data were recorded on a phantom head, whereas in the second experiment a validation was made on real MEG data collected on a healthy human subject. In both cases, we compared our results with those obtained with classical multiple dipoles methods for source localization. For EEG data, the brain electrical source analysis (BESA) implementation (MEGIS Software Gmbh, Munich, Germany) was chosen, and for MEG data DipoleFit software (CTF Systems, Inc., Vancouver, Canada) was used. We also compared these results to those obtained with a minimum-norm solution with and without multiresolution. We could not compare our results with those obtained with the anatomy-based original nonlinear regularization without the multiresolution process because of computational difficulties. In both cases, the forward problem was computed in a spherical head model.

A. Results From a Phantom Head

The phantom head is a dry human skull filled with solidified saline gelatin. Six current sources made of coaxial cables embedded in thin glass tubes were put in the head volume (see [16] for more details). Data were acquired from 60 electrodes uniformly distributed over the scalp surface, see Fig. 3. A virtual cortex mesh was adapted to the head volume and to the six sources locations to enable source estimation with cortically distributed methods.

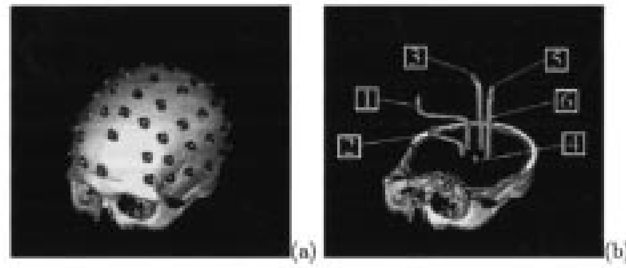

Fig. 3. (a) A three-dimensional (3-D) view of the registered 60 electrodes on the skull. (b) A 3-D view of the sources with their positioning tubes.

TABLE I
Spatio-Temporal Dipole Fit With BESA on Phantom: Localization Error

Sources	1	2	3	4	5	6	<>
$\epsilon(cm)$	1.19	1.28	1.34	1.94	0.67	1.06	1.25

TABLE II
Minimum-Norm Results on Phantom Without Multiresolution: Localization Errors

Sources	1	2	3	4	5	6	<>
$\epsilon_{max}(cm)$	1.11	2.17	1.54	6.40	0.97	2.61	2.47
$\epsilon_G(cm)$	2.17	3.86	4.02	4.19	2.48	2.54	3.21

TABLE III
Spatio-Temporal Fit on Phantom Using a Minimum-Norm Estimation With Multiresolution

Sources	1	2	3	4	5	6	<>
$\epsilon_{max}(cm)$	0.96	2.69	2.15	4.59	0	1.19	1.93
$E_{max}(\%)$	57.5	20.8	34.3	80.5	52.7	61.7	51.2
$\epsilon_G(cm)$	0.73	1.65	2.65	3.36	0.25	1.28	1.65

The results obtained by BESA are shown in Table I, where ϵ is the localization error. They are acceptable since we obtained an average localization error of 1.25 cm. Only source number four was poorly reconstructed (1.94 cm) due to its great depth in the skull.

The results obtained with minimum-norm regularization, without multiresolution are displayed in Table II. $\epsilon_{\max}$ is the distance between the real source and the source of maximal amplitude, whereas ϵ_G is the distance between the real source and the center of gravity of activity in the reconstructed distribution. $E_{\max}$ is the percentage of the source distribution energy contained in the maximal amplitude source. These results showed that maximal amplitude sources were badly recovered: 2.47 cm on average. Moreover, the activity was widespread with a center of gravity that was far from the maximal amplitude source, leading to difficulties in interpreting the reconstructed distribution.

Table III shows the results obtained with the same minimum-norm regularization but with the multiresolution process. Reconstruction was slightly improved (between 1.5 and 2 cm on average) and more focal, with an average of about fifty percent of the total energy in the maximal amplitude source.

TABLE IV
SPATIO-TEMPORAL FIT ON PHANTOM USING A BAYESIAN ESTIMATION WITH MULTIRESOLUTION

Sources	1	2	3	4	5	6	<>
$\epsilon_{max}(cm)$	0.39	0	2.71	1.23	0	1.21	0.9
$E_{max}(\%)$	100	54.5	100	100	100	47.9	83.7
$\epsilon_G(cm)$	0.39	0.85	2.71	1.23	0	1.90	1.18

TABLE V
RESULTS FROM HUMAN MEG DATA WITH A MINIMUM-NORM REGULARIZATION WITHOUT MULTIRESOLUTION COMPARED WITH DIPOLAR METHOD RESULTS

Digits	1	2	3	4	5	<>
$\epsilon_{max}(cm)$	9.19	9.50	9.11	9.31	9.24	9.27
$E_{max}(\%)$	1.9	1.0	1.87	1.34	0.86	1.39
$\epsilon_G(cm)$	3.50	4.43	4.99	4.48	4.83	4.45
Number of active sources	256	236	242	235	225	239

TABLE VI
RESULTS FROM HUMAN MEG DATA WITH A MINIMUM-NORM REGULARIZATION WITH MULTIRESOLUTION COMPARED WITH DIPOLAR METHOD RESULTS

Digits	1	2	3	4	5	<>
$\epsilon_{max}(cm)$	1.46	5.68	3.69	1.26	1.03	2.62
$E_{max}(\%)$	15.2	8.9	24.1	9.8	18.7	15.3
$\epsilon_G(cm)$	2.43	1.45	4.23	3.17	2.22	2.70
Number of active sources	79	136	18	52	112	79

TABLE VII
MULTIRESOLUTION RESULTS FROM HUMAN MEG DATA WITH A BAYESIAN REGULARIZATION COMPARED WITH DIPOLAR METHOD RESULTS

Digits	1	2	3	4	5	<>
$\epsilon_{max}(cm)$	2.35	1.27	0.95	1.16	0.91	1.33
$E_{max}(\%)$	91.4	15.7	41.8	51.3	18.0	43.6
$\epsilon_G(cm)$	2.18	0.31	0.55	1.40	1.64	1.22
Number of active sources	12	54	27	30	46	34

Nevertheless, only the use of a nonquadratic regularization procedure included into a multiresolution process allowed a precise and focal localization of the source, see Table IV: about 1 cm for the localization error and 83.7% for $E_{\max}$. Noticeably, the deeper source (number 4) was correctly recovered.

B. Results on Real Data

In this experiment, the multiresolution method is evaluated on real MEG data recorded on a healthy human subject (CTF MEG system with 151 channels, Paris), in a somatosensory experiment. We recorded the magnetic brain response to an electric stimulation of the digits. The purpose was to map the cortical representation of the fingers of right hand of the subject and to compare it with prior anatomical knowledge about somatotopy and with dipolar method results.

The results obtained with a simple minimum-norm constraint, without multiresolution are presented in Table V. Like above, the error $\epsilon_{\max}$ is the distance between the source of maximal amplitude and the dipole identified by DipoleFit and ϵ_G is the distance to the center of gravity. We also give the number of sources that had significant amplitude, i.e., an amplitude two standard deviations above that of the reconstructed distribution. In this case, more than 4 and 9 cm were found between the dipole identified by dipolar fit (DipoleFit software, CTF Syaytems, Inc., Vancouver, Canada) and the maximal amplitude source and the center of gravity, respectively. Clearly, these results are unconsistent. But when minimum-norm regularization was integrated into a multiresolution procedure, consistent with DipolEFit's results were obtained, see Table VI. The interpretation of the obtained distribution is nonetheless problematic given the large number of sources with significant amplitude—79 on average—and the widespread activity. Indeed, the maximal amplitude source contained only 15% of the total energy. Results obtained with the multiresolution process combined with nonquadratic regularization to the DipoleFit results are given in Table VII. This method yielded 45% of the total energy in the maximal source and 34 significant sources on average.

The projection of the reconstructed dipoles on a 3-D reconstruction of the white and gray matters interface is shown in Fig. 4. They indicate a good anatomical localization of sensory primary areas.

IV. DISCUSSION AND CONCLUSION

Distributed source models have proven to be an interesting direction for extracting realistic images of task-related neuronal networks from EEG/MEG data, but suffer from large source space dimensions and bad conditioning of the linear operator. To counter this limitation, we have developed a multiresolution method, combined with a realistic regularization based on the anatomy of the subject. This approach was validated in two different experiments. In the first one, six sources of known locations were successively activated in a phantom head, and then reconstructed from surface EEG. The second experiment aimed at mapping the hand's representation on the cortex from MEG data. In both cases, we confronted the results obtained with a nonquadratic regularization integrated into a multiresolution scheme with a dipolar method, a distributed source model used with a constraint of minimal norm and no multiresolution, and a distributed source model used with a constraint of minimal norm integrated into a multiresolution scheme. The results showed that the multiresolution procedure always yielded a solution that was more focal and realistic than without multiresolution.

In both experiments, classical dipolar methods produced reasonable results. However, these methods require some prior knowledge on the number of dipoles to fit, i.e., the number of activated areas in the brain. In the phantom experiment case, we successively activated one dipole at a time. Accordingly, a single dipole position and orientation were fitted, as in the second experiment when the cortical representation of one digit was to be reconstructed. The presence of multiple local minima in the criteria to be minimized during the localization procedure of multiple dipoles also induces sensitivity of dipolar methods to initialization. In most cases, prior knowledge on activity localization is, therefore, also required. In conclusion, dipolar methods are here presented for comparison because of their wide use in the source localization EEG/MEG inverse problem, but cannot be considered as a validation.

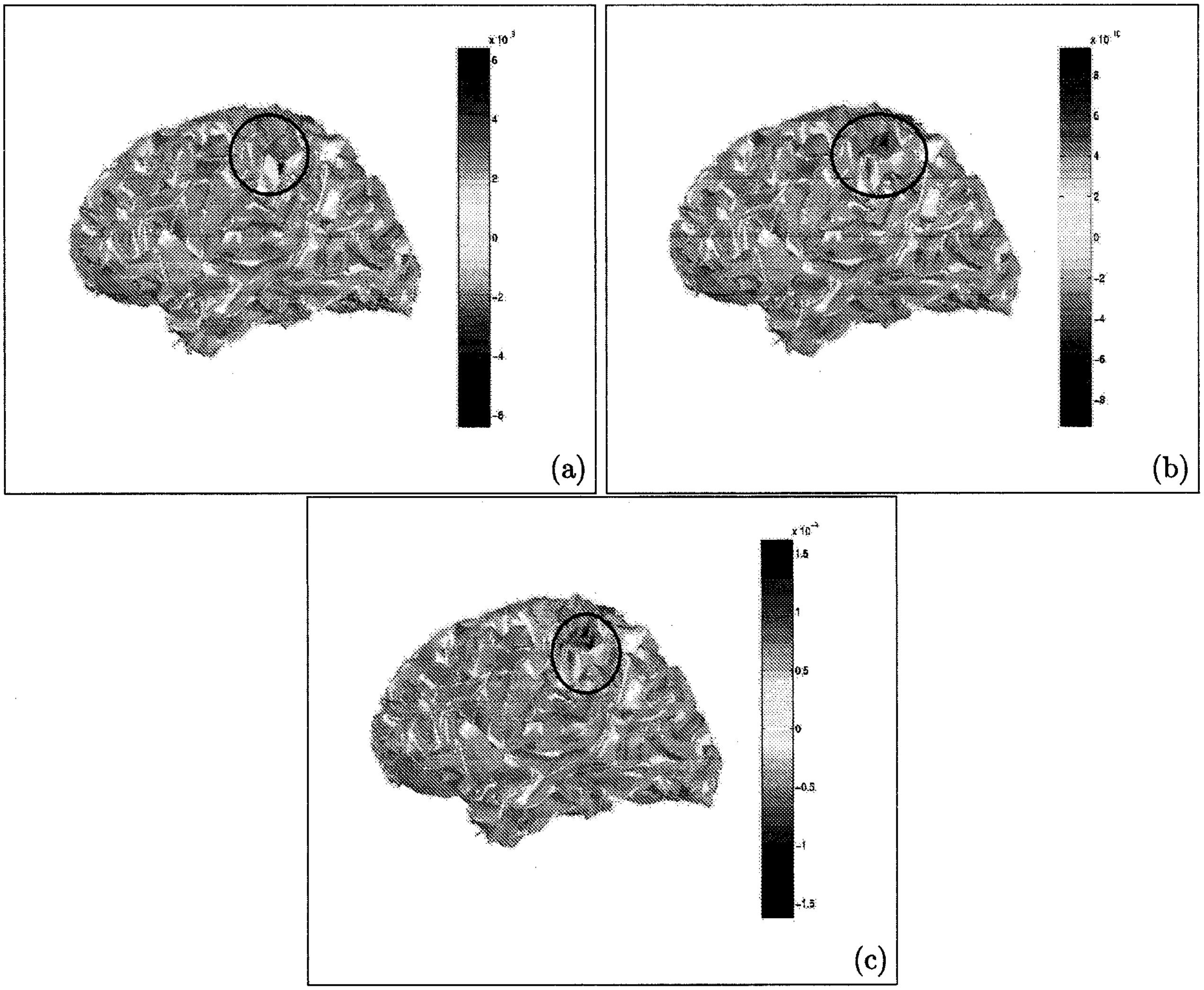

Fig. 4. The cortical representation of (a) right thumb, (b) right forefinger, and (c) right little finger projected onto a 3-D reconstruction of the cortex from the structural MRI.

Results obtained with a minimum-norm constraint and no multiresolution were clearly not realistic with a very widespread activity all over the cortex. When the minimum-norm constraint was integrated into a multiresolution scheme, reconstruction was slightly improved but was still widespread around the activity focus. Therefore, a primary conclusion is that only some anatomy-based regularization integrated into a multiresolution procedure allows focal and comparable results in terms of localization to dipolar method, without requiring any prior knowledge on the number of activity centers and on the activity location.

On the other hand, an interesting clinical implication of the results from the multiresolution method is that, contrary to dipolar methods, activation fields are explicitly recovered along the cortical surface. This is consistent with the spatial extension of the functional maps drawn by electrophysiological studies performed on animals, [17].

In conclusion, the multiresolution approach appears to be a very promising attempt at upgrading EEG/MEG to the level of a true brain imaging technique. With poor regularization of the inverse problem, the multiresolution procedure would be prone to mislocalizations and widespread oversmoothing. This justifies the association with an anatomy-based nonquadratic regularization technique. Future developments should concentrate on the quantification of the spatial extension of activity on the cortical surface.

ACKNOWLEDGMENT

The authors would like to thank Dr. J. Idier for his precious advice on regularization techniques. They would also like to thank D. Papo for valuable suggestions and comments on the manuscript.

REFERENCES

[1] S. Baillet and L. Garnero, "A Bayesian approach to introducing anatomo-functional priors in the EEG/MEG inverse problem," *IEEE Trans. Biomed. Eng.*, vol. 44, pp. 374–385, May 1997.

[2] M. Scherg and D. von Cramon, "Evoked dipole source potentials of the human auditory cortex," *Electroencephalogr. Clin. Neurophysiol.*, vol. 65, pp. 344–360, 1986.

[3] M. Hämäläinen and R. Llmoniemi, "Interpreting measured magnetic fields of the brain: Estimates of current distributions," Helsinki Univ., Helsinki, Finland, Tech. Rep. TKK-F-A620, 1984.

[4] R. Pascual-Marqui *et al.*, "Low resolution electromagnetic tomography: A new method for localizing electrical activity of the brain," *Int. J. Psychophysiol.*, vol. 18, pp. 49–65, 1994.
[5] A. Dale and M. Sereno, "Improved localization of cortical activity by combining EEG and MEG with MRI cortical surface reconstruction: A linear approach," *J. Cogn. Neurosci.*, pp. 162–176, 1993.
[6] J. W. Phillips, R. M. Leahy, and J. C. Mosher, "MEG-based imaging of focal neuronal current sources," *IEEE Trans. Med. Imag.*, vol. 16, pp. 338–348, June 1997.
[7] I. Gorodnistky, J. George, and B. Rao, "Neuromagnetic imaging with FOCUSS: A recursive weighted minimum-norm algorithm," *Electroencephalogr. Clin. Neurophysiol.*, vol. 95, pp. 231–251, 1995.
[8] P. Valdes-Sosa, F. Marti, F. Garcia, and R. Casanova, "Variable Resolution Electric-Magnetic Tomography," in *Biomag 96': Proceedings of the Tenth International Conference on Biomagnetism*. New York: Springer-Verlag, 2000, vol. II.
[9] R. Srebro, "An iterative approach to the solution of the inverse problem," *Electroencephalogr. Clin. Neurophysiol.*, vol. 98, pp. 349–362, 1996.
[10] S. Baillet, "Vers une imagerie fonctionnelle de l'électrophysiologie corticale. Modélization markovienne pour l'estimation des sources de l'électro/magnétoencéphalographie et évaluations expérimentales," Ph.D. dissertation, Université de Paris-Sud, Orsay, France, July 1998.
[11] A. Tikhonov and V. Arsenin, *Solutions of Ill-Posed Problems*. Washington, DC: Winston, 1977.
[12] S. Geman and D. Geman, "Stochastic relaxation, Gibbs distributions, and the Bayesian restoration of images," *IEEE Trans. Pattern Anal. Machine Intell.*, vol. PAMI-6, pp. 721–741, Nov. 1984.
[13] G. Demoment, "Image reconstruction and restoration: Overview of common estimation structure and problems," *IEEE Trans. Acoust. Speech, Signal Processing*, vol. 37, pp. 2024–2036, Dec. 1989.
[14] J. Idier, "Regularization tools and models for image and signal reconstruction," in *Proc. 3rd Int. Conf. Inverse Problems in Engineering*, Port Ludlow, WA, June 1999, pp. 1–6.
[15] P. Charbonnier, L. Blanc-Féraud, and M. Barlaud, "Deterministic edge-preserving regularization in computed imaging," *IEEE Trans. Image Processing*, vol. 6, pp. 298–311, Feb. 1997.
[16] S. Baillet, J. Riera, L. Garnero, G. Marin, J. Mangin, and J. Aubert, "Evaluation of inverse methods and head models for EEG source localization using a human skull phantom," *Phys. Med. Biol.*, submitted for publication.
[17] Y. Iwamura, M. Tanaka, M. Sakamoto, and O. Hikosaka, "Functional subdivisions representing different finger regions in area 3 of the first somatosensory cortex of the conscious monkey," *Exp. Brain Res.*, vol. 51, pp. 315–326, 1983.

Laurence Gavit was born in France, on August 30, 1974. From 1993 to 1998, she was a student at Ecole Supérieure d'Ingénieurs en Electrotechnique et Electronique of Paris, France, where she received the engineer degree in Signal Processing and Telecommunications in 1998. She received the Ph.D. degree in Signal Processing from the University of Paris XI (Orsay) in 2001.

During her Ph.D. degree program, she worked at La Salpêtrière Hospital, in the laboratory of Cognitive Neurosciences and Brain Imaging, on the reconstruction of brain electrical activity from electroencephalography (EEG) or magnetoencephalography (MEG). She is now with the Imaging group at General Electric Medical Systems, Buc, France

Sylvain Baillet (M'00) was born in France in 1970. He graduated in Applied Physics from the Ecole Normale Supérieure, Cachan and in Signal Processing from the University of Paris-Sud, in 1994. In 1998, he completed the Ph.D. program in Electrical Engineering from the University of Paris-Sud at the Institute of Optics, Orsay, and at the Cognitive Neuroscience and Brain Imaging Laboratory at La Salpêtrière Hospital, Paris. From 1998 to 2000, he was a Post-Doctoral Research Associate with the NeuroImaging group at the Signal and Image Processing Institute, University of Southern California, Los Angeles.

He is now a research scientist with the National Center for Scientific Research (CNRS) and the Cognitive Neuroscience and Brain Imaging laboratory, La Salpêtrière Hospital. His research interests primarily concern methodological and modeling issues in functional brain imaging.

Jean-François Mangin received the engineer degree from Ecole Centrale Paris in 1989, the M.Sc. degree in numerical analysis from Pierre et Marie Curie University (Paris VI) in 1989, and the Ph.D. degree in signal and image processing from Ecole Nationale Superieure des Telecommunications of Paris in 1995.

Since 1991, he has been working with the Service Hospitalier Frederic Joliot of the CEA Medical Research Department. Since 1999, he has been leading a group, which project consists of the development of a brand-new bunch of brain mapping methods designed from a structural point of view. The main goals are the inference of a generic model of the cortical folding pattern that explains inter-individual variability, and the inference of the cortex connectivity from diffusion-weighted magnetic resonance imaging. The underlying methodological domains are Mathematical Morphology, Markovian Random Fields and Graph Theory.

Jérémie Pescatore was born in London, U.K., on February 1974. He received the M.Sc. degrees in electrical engineering and image processing from the National Institute of Applied Sciences (INSA) in Lyon (France) in 1998.

He spent six months in 1997 as a research assistant at the NMR unit of the Institute of Neurology in London, United Kingdom working on medical registration. He worked in 1998 at the LIMSI studying Man–Machine-Communication applied to Telemedecine. He is currently preparing a Ph.D. degree in biomedical medical imaging in the Signal and Image Processing Group (TSI) at the Ecole Nationale Superieure des Telecommunications (ENST) in Paris, France in collaboration with the LENA and the MEG center at the Pitie-Salpetriere Hospital. He research interests concern finite element meshes, MEG, EEG, discrete geometry, topology, registration, medical signal and image processing and man–machine communication.

Line Garnero (M'00) was born in France, on September 4, 1955. She received the Doctorat de 3ème Cycle and the Doctorat d'Etat from the University of Paris XI (Orsay) in 1981 and 1987, respectively.

She is Directeur de Recherche at the CNRS (National Center of Scientific Research). She worked at the Institute of Optics in Orsay from 1981 to 1996. Her research field was the image reconstruction techniques for microwave, X ray or tomography. She works now in the laboratory of Cognitive Neurosciences and Cerebral Imaging in La Salpêtrière Hospital, Paris, where her main research concerns the reconstruction of brain electrical activity from electroencephalography (EEG) or magnetoencephalography (MEG).